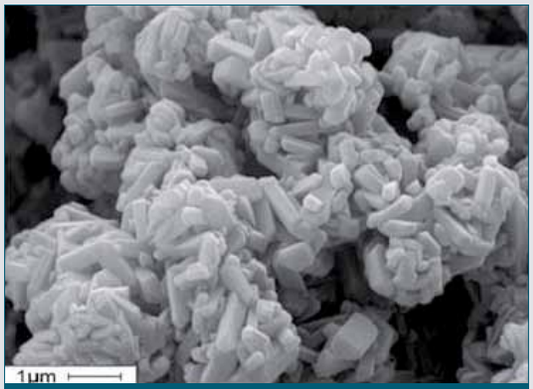

Fig. 1 - SEM image of YPO_4:Tb

Fabio Angiuli, Enrico Cavalli
Dipartimento di Chimica Generale ed Inorganica
Università di Parma
fabioangiu@yahoo.it

LUMINESCENCE PROPERTIES AND EMISSION DYNAMICS OF YPO_4 ACTIVATED WITH Tb^{3+} AND Bi^{3+}

The synthesis of YPO_4 both singly doped with Tb^{3+} and co-doped with Bi^{3+} has been carried out by the Pechini sol-gel method and solid state reaction. Good quality materials have been obtained in terms of particle size, morphology and of emission performance. The co-doping with Bi^{3+} results in a significant increase of the luminescence intensity even upon direct rare earth excitation. The excited states dynamics of these phosphors have been discussed by taking into consideration the effect of the presence of Bi^{3+} on the optical properties of the host lattice.

Introduction

YPO_4 is an attractive host lattice for trivalent rare earth ions thanks to its favorable physico-chemical properties like high and extended transparency, thermal and chemical stability, structural characteristics, and it is extensively investigated in order to develop phosphors for solid state lighting, PDP technology, etc. [1]. In this work we deal with the spectroscopic properties of YPO_4 activated with Tb^{3+} and the effect of the Bi^{3+} co-doping on the emission performances of these systems. The yttrium phosphate lattice is very suitable for this kind of study since its large bandgap and the absence of host-rare earth energy transfer facilitate the study of the role of the co-doping ion in the sensitization of the rare earth luminescence.

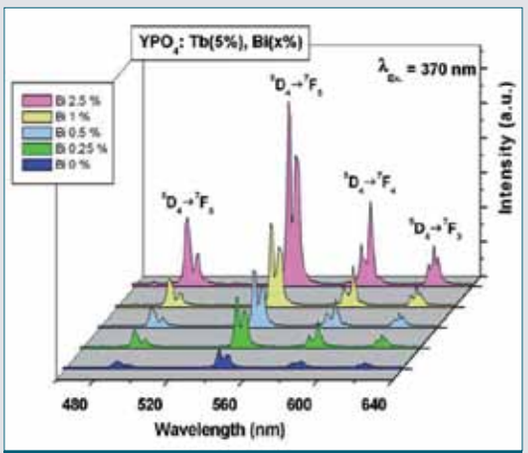

Fig. 2 - YPO_4:Tb emission spectra

Materials

The phosphors used in this study have been synthesized by the Pechini sol-gel method and solid state reaction. They have been characterized by X-ray diffraction and scanning electron microscopy (SEM). The obtained compounds are single phase and constituted by particles with well defined elongated shape and size distribution in the 200-800 nm range (Fig. 1).

Results and conclusions

The luminescence spectra of the YPO_4:Tb^{3+}(5%), Bi^{3+}(x%) phosphors measured upon direct Tb^{3+} excitation at 370 nm are shown in Fig. 2. They are constituted of transitions originating in the $^5D_4$(Tb^{3+}) emitting level, whose intensity progressively increases with the Bi^{3+} concentration. In addition it has been observed that: i) the excitation band at 234 nm corresponding to the Bi^{3+} absorption is weak, indicating that the Bi^{3+}→Tb^{3+} energy transfer process is not very efficient; ii) in addition, the decay time of the $^5D_4$ emission decreases as the Bi^{3+} concentration increases. This behavior indicates an increase of the radiative emission probability with the co-doping level, that we have associated to the increment of the refractive index induced by the progressive substitution of Bi^{3+} for Y^{3+} [2]. This qualitative model has then been confirmed by experiments on other YPO_4:RE^{3+}, Bi^{3+} (RE= Sm, Eu, Nd) phosphors.

References

[1] H. Lai *et al., J. Chem. Phys. C*, 2008, **112**, 282.
[2] A.S. Korotkov, V.V. Atuchin, *Opt. Comm.*, 2008, **281**, 2132.

RIASSUNTO

Proprietà di luminescenza e dinamiche di emissione dell' YPO_4 attivato con Tb^{3+} e Bi^{3+}

L'YPO_4 singolarmente attivato con Tb^{3+} e codrogato con Bi^{3+} è stato sintetizzato sia con la tecnica sol-gel che con la reazione a stato solido, ottenendo materiali con buona qualità in termini di morfologia delle particelle e prestazioni di emissione. Il codrogaggio con Bi^{3+} induce un significativo aumento dell'intensità della luminescenza anche eccitando direttamente nel Tb^{3+}.

Il presente contributo è stato presentato alla XII Giornata della Chimica dell'Emilia Romagna, svoltosi il 17 dicembre 2012 presso il Dipartimento di Scienze Chimiche e Farmaceutiche dell'Università di Ferrara.

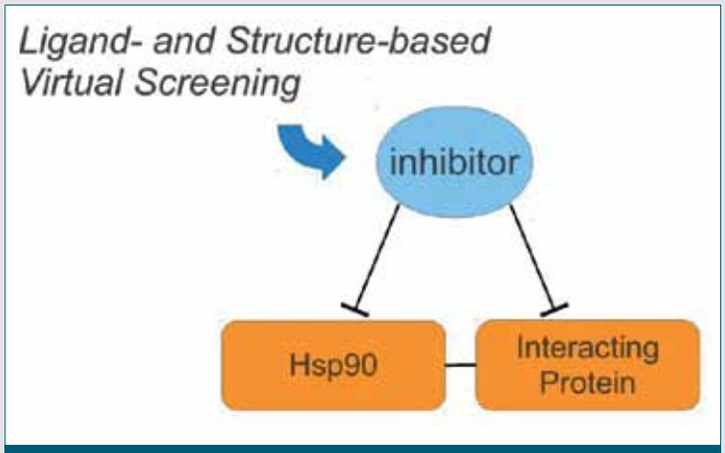

Schematic representation of the aim of the project: use of combined ligand- and structure-based virtual screening techniques to discover potential multi-target inhibitors of the Hsp90 interactome

*Andrew Anighoro[1], Dagmar Stumpfe[2], Kathrin Heikamp[2], Jürgen Bajorath[2], Giulio Rastelli[1]**
[1]Dipartimento di Scienze della Vita
Università di Modena e Reggio Emilia
[2]Department of Life Science Informatics
B-IT, LIMES Program Unit Chemical Biology
and Medicinal Chemistry
Rheinische Friedrich-Wilhelms-Universität (Bonn, D).
andrew.anighoro@unimore.it

RICERCA

TARGETING THE HSP90 INTERACTOME USING IN SILICO POLYPHARMACOLOGY APPROACHES

Hsp90 and its interactome represent an attractive array of targets for polypharmacological drug design strategies in cancer therapy. In this work, we propose a computational protocol aimed at the selection of promising target combinations and potential multi-target active compounds.

Introduction

In recent years, polypharmacology has gained popularity in drug discovery [1]. Especially for complex diseases such as cancer, the ability of a drug to bind to and interfere with multiple targets provides new opportunities for therapeutic intervention. In this article, we focus on Hsp90 and its interactome, whose pivotal role in survival and proliferation of cancer cells renders this array of targets particularly attractive for polypharmacological drug design strategies.

The primary goal of our work is the identification and selection of suitable target proteins from the interactome that might be combined with Hsp90 to explore and exploit a multi-target inhibition approach. This task is accomplished by applying computational methods to mine the structural and biological information associated with potential ligands in public databases and assess the degree of structural similarity between known inhibitors of different targets. Therefore, we propose an integrated ligand- and structure-based approach to select small molecules from databases suitable for consideration as multi-target inhibitors.

Biological background

Cancer is one of the world leading causes of death accounting for 7.6 million deaths in the year 2008. The number of deaths per year is projected to rise to 13.1 million in 2030 [2]. Both genetic and environmental factors may be at the origin of human cancers. In general, cancer cells are characterized by uncontrolled proliferation and survival. Indeed, several cellular pathways might be affected by this pathology contributing to the expression of the transformed phenotype. Heat shock response is often activated in cancer cells, contributing to both initiation and maintenance of the transformed phenotype. Hsp90 is an important component of this process, acting as a molecular chaperone affecting stability and activation of more than 200 client proteins through ATP hydrolysis cycles [3]. Proteins interacting with Hsp90 are often involved in signalling processes, such as transcription factors and kinases.

Polypharmacology and Hsp90

Popular computational methods applied in medicinal chemistry include ligand- and structure-based virtual screening. These techniques aim at finding new small organic molecules with specific activity against a given biological target. Typically, the target is a protein that might act as an enzyme, a receptor, or an ion-channel, whose activity is involved in a pathological mechanism. The interaction of the small molecule with the target is intended to interfere with the protein's activity in a physiologically relevant manner. Following the classical drug design paradigm, the small molecule should be highly selective for the chosen target. Interactions with additional targets might be the cause of the so called off-target effects, which in turn might be responsible for toxicity and thus impair the development of a safe, marketable drug.

Il presente contributo è stato presentato alla XII Giornata della Chimica dell'Emilia Romagna, svoltosi il 17 dicembre 2012 presso il Dipartimento di Scienze Chimiche e Farmaceutiche dell'Università di Ferrara.

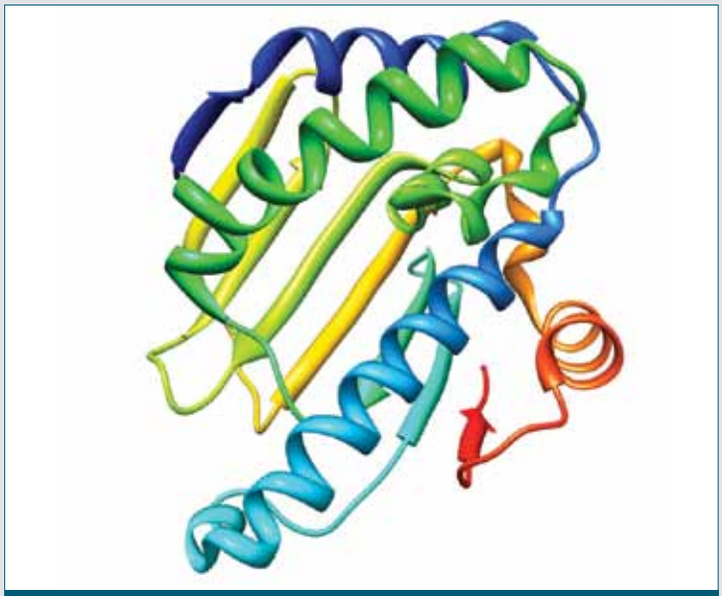

An X-ray crystal structure of Hsp90

The idea of targeting multiple proteins involved in a given pathology was initially applied by prescribing multiple drugs in combination therapies. Nevertheless, some drugs initially designed to be target-selective have been proven later on to exert their therapeutic activity through the simultaneous interaction with multiple targets. Hence, the paradigm of trying to design drugs acting on a single target has recently been extended by the concept of polypharmacology, which aims at rationally develop therapeutic agents that interact simultaneously with multiple targets. In principle, this approach has the advantage that it could cause an improved therapeutic effect and bypass complications associated with the prescription of two or more drugs in combination therapies. Designing compounds acting on multiple targets is a complex task but, if successful, might often lead to more efficient drugs (in therapeutic areas where target specificity is not a stringent requirement). In this context, a key question is which combination(s) of targets should best be considered for a polypharmacology approach to treat a particular disease.

Given the pivotal role on Hsp90 in cancer, the development of Hsp90 inhibitors has long been a major focal point in oncological drug discovery [4, 5]. The most important chemical classes of Hsp90 inhibitors include, among others, ansamycins, resorcinol derivatives, purines, imidazopyridines, oxazoles. Fourteen drug candidates targeting Hsp90 are now undergoing clinical trials, but none of them has as of yet achieved market approval.

Because Hsp90 is a key node in many biological networks and interacts with a very large number of client proteins and co-chaperones [4], this target and its interactome are thought to be highly relevant for polypharmacology approaches. However, polypharmacological approaches to target Hsp90 are still largely unexplored.

Workflow and results

For rational polypharmacological ligand design targeting the the Hsp90 interactome, a computational procedure has been designed that consists of several steps, the first of which is an activity annotation analysis in public compound databases to collect known inhibitors of Hsp90 and its client proteins.

So identified inhibitors have been used as templates for ligand-based virtual screening of the ChEMBL [6] and ZINC [7] databases. Then, the analysis of the top-ranked database compounds taking activity annotations as well as implications of their targets in cancer into account led to the selection of most promising candidates for interference with Hsp90 in combination with secondary targets. For each target combination selected, a focused compound library has been built with the purpose of finding new multi-target active compounds without any known target annotation. Finally, structure-based virtual screening of these focused libraries against Hsp90 and the secondary targets has been carried out to further refine the selection and evaluate more thoroughly the potential affinity of pre-selected compounds.

Conclusions

The analyses conducted so far suggest that public molecular databases contain a wealth of information about compounds active against the Hsp90 interactome. We have analyzed this information comprehensively and utilized it to design a computational polypharmacological approach. Following our approach, suitable target combinations have been identified and integrated ligand- and structure-based virtual screening applied to identify candidate compounds for multi-target inhibition. Importantly, our computational approach to Hsp90 polypharmacology will be complemented by experimental evaluation of candidates and subsequent iterations of integrated virtual screening.

References

[1] A.D. Boran, R. Iyengar, *Curr. Opin. Drug Discov. Devel.*, 2010, **13**(3), 297.
[2] J. Ferlay *et al., Int. J. Cancer.*, 2010, **127**(12), 2893.
[3] J. Trepel *et al., Nature Reviews Cancer*, 2010, **10**, 537.
[4] M. Sgobba, G. Rastelli, *ChemMedChem*, 2009, **4**, 1399.
[5] P.C. Echeverría *et al., PLoS ONE*, 2011, **6**(10), e26044.
[6] A. Gaulton *et al., Nucleic Acids Res.*, 2012, **40**, D1100.
[7] J.J. Irwin, B.K. Shoichet, *J. Chem. Inf. Model.*, 2005, **45**(1), 177.

RIASSUNTO

Approcci polifarmacologici in silico mirati all'interattoma di Hsp90

Hsp90 ed il suo interattoma sono bersagli attraenti per l'applicazione di strategie polifarmacologiche nella terapia antitumorale. In questo studio viene proposto un protocollo computazionale mirato alla selezione di combinazioni promettenti di bersagli e di potenziali composti attivi su bersagli multipli.

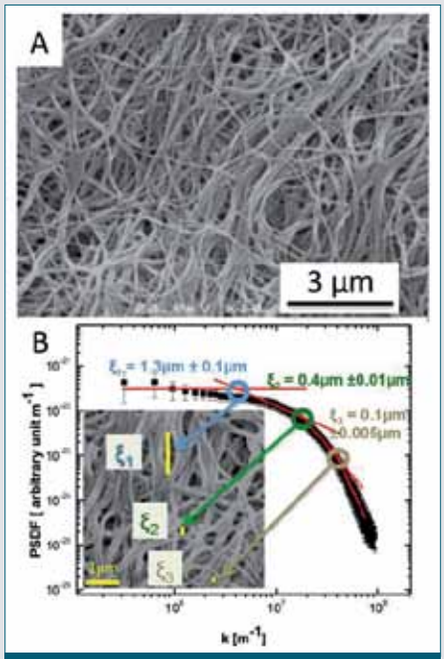

Fig. 1 - A) SEM image of fibrin network; B) PSDF

Marianna Barbalinardo[1,2], Francesco Valle[1], Beatrice Chelli[1], Eva Bystrenova[1], Giulia Foschi[1], Elettra Zanotto[2], Giuseppe Falini[2], Graziella Pellegrini[3], Fabio Biscarini[1]
[1]CNR- Istituto per lo Studio dei Materiali Nanostrutturati Bologna
[2]"Alma Mater Studiorum" Università di Bologna
[3]Center for Regenerative Medicine "Stefano Ferrari" Università di Modena and Reggio Emilia
mbarbalinardo@bo.ismn.cnr.it

FABRICATION, CHARACTERIZATION AND POROSITY ANALYSIS OF A SCAFFOLD BASED ON FIBRIN GLUE

Fabrication of fibrin scaffolds for the regeneration of tissues. The characterization of the fibrin network is crucial for evaluating its morphology, porosity and biological efficacy, thus we characterized the fibrin by scanning electron microscopy.

Introduction

Tissue engineering combines cell and molecular biology with materials and nanotechnology to repair or improve the biological functions of tissues that are damaged or ceased to perform their task. A key component for tissue regeneration is the scaffold that serves as a template for cell growth and interactions and for the formation of the structural support to the newly formed tissue. Scaffolds should be biocompatible or biodegradable, nontoxic, non-immunogenic and should display a structure, usually porous, allowing the cell adhesion, migration and the exchange of molecules required as nutrients or signalling. There are many natural (collagen, fibrin, alginate and chitosan) and synthetic polymers [3] that have been used to this aim. Fibrin is a critical blood component responsible for haemostasis, and it is widely used in biomedical field, as it is highly compatible with tissues, it is biodegradable and it has no toxic properties. Fibrin alone or in combination with other materials has been used as a biological scaffold for stem or primary cells to regenerate adipose tissue, bone, cardiac tissue, cartilage, liver, nervous tissue, ocular tissue, skin, tendons and ligaments. Thus, fibrin is a versatile biopolymer, displaying a great potential in tissue regeneration and wound healing. The performance of fibrin sealant has been extensively described. The goals of this study are two-fold: 1) the fabrication of a fibrin scaffold easy to be handled; 2) the fabrication of a film with pore size sufficiently large to allow the cell nutrition flow and at the same time small enough not to allow the cells to pass over the film.

Materials and Methods

Standing fibrin gel film preparation

Fibrin gel was prepared from a 0.5 ml kit of Tissucol® (Baxter, Wien, Austria) composed of 70-110 mg fibrinogen and 500 U.I. thrombin stock solutions. We diluted the solution of fibrinogen at an initial concentration of 40 mg/ml, the initial concentration of thrombin was 3 U.I.

The same volumes of the two solutions were mixed in an eppendorf tube. After substrate cleaning, the glass was coated with a thin Teflon-AF. A drop of fibrin gel solution was placed on the substrate in the centre of a confining polydimethylsiloxane (PDMS) frame fabricated by photolitograhy and replica molding.

Then, another glass surface was placed on the fibrin drop, without additional pressure on the upper surface. The sample was incubated 24 hours at 4 °C. The result was a fibrin gel. After the incubation time the surface of the glasses were removed, and in this way a film of fibrin easy to handle was obtained.

Preparation of Teflon-Af films

Teflon-AF (Sigma Aldrich) was dissolved in Fluorinert FC-40 (Sigma Aldrich) at concentration of 16.5 mg/mL at room temperature; the solution was then spin-coated onto the glass substrates by a Laurell Technologies Corporation Spin Coater (30", acc. 400, 5000 r.p.m.).

The final, contact angle of the Teflon-AF coated glass with milliQ water was 105° [1].

Il presente contributo è stato presentato alla XII Giornata della Chimica dell'Emilia Romagna, svoltosi il 17 dicembre 2012 presso il Dipartimento di Scienze Chimiche e Farmaceutiche dell'Università di Ferrara.

Preparation of the fibrin scaffold for scanning electron microscopy (SEM)

Prior SEM imaging the fibrin scaffold were fixed in 2.5% gluteraldehyde in phosphate buffered saline (PBS) buffer at 4 °C, for 1 hour. Each sample was then rinsed three times in PBS for 5 minutes before being incubated for 1 hour with 1% osmium tetra-oxide (OsO_4). The samples were rinsed 3 times with distilled water 10 minutes each time. Then samples were sequentially dehydrated in 75%, 95% and 99% ethanol. The SEM procedures were finished by gold coating. Then the samples were mounted on the SEM sample holder and examined using a Hitachi S4000F FEG-SEM.

Scaffold Morphology

One goal of these studies was to fabricate three-dimensional scaffold with well-define morphology. We employed SEM to qualitatively and quantitatively assess the physical architecture of the scaffolds. Fig. 1a shows the network of fibrin confined in the PDMS frame. To understand the morphology of fibrin network we calculated the Power Spectrum Density (PSDF). From this plot (Fig. 1b) we can identify three correlation lengths ξ_1, ξ_2 and ξ_3 corresponding to changes in the slope of the PSDF in logarithmic scales, representing the characteristic lengths of the fiber network (fiber size, spacing) [2].

Conclusions

In this work, we have demostrated the realization of a fibrin scaffold, of different thickness and easy to handle fabricated under confinement.
The characterization of the fibrin network by SEM has helped us to understand how the morphology of fibrin network might affect the cell growth. In fact the different correlation lengths are important because they must fit important requirements for the cell proliferation: large enough to bring the nutrition and small enough to allow the development of multiple points of adhesion for each cell (cell 5-10 μm).

References

[1] F. Valle *et al., Advanced Biomaterials*, 2010, **12**, 85.
[2] A. Calò *et al., J. Phys. Chem. B*, 2009, **113**, 4987.
[3] S. Van Vlierberghe *et al., Biomacromolecules*, 2011, **12**, 1387.

RIASSUNTO

Fabbricazione, caratterizzazione e analisi di supporti di fibrina

Fabbricazione di supporti di fibrina per la rigenerazione dei tessuti. La fibrina forma un complicato intreccio di fibre. La caratterizzazione del network è fondamentale per valutare la morfologia, la porosità e l'adesione cellulare.

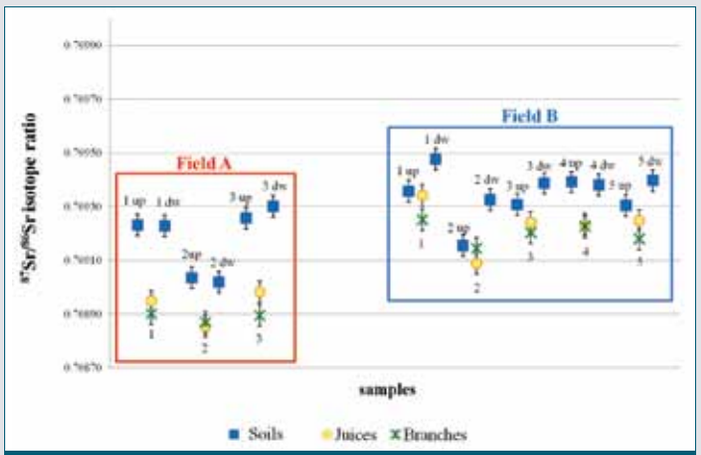

Fig. 1 - $^{87}Sr/^{86}Sr$ isotope ratios relative to soil samples extracted with NH_4NO_3, vine branches and grape juices of two fields of the Lambrusco wine pilot study

Lucia Bertacchini, Michele Silvestri, Caterina Durante, Marina Cocchi, Andrea Marchetti
Dipartimento di Scienze chimiche e geologiche
Università di Modena e Reggio Emilia
lucia.bertacchini@unimore.it

GEOGRAPHICAL TRACEABILITY STUDIES FOR THE OENOLOGICAL CHAIN VALORISATION

The possibility to find out objective criteria for the geographical traceability of food is a challenging task, which could have important effects from an economic and social standpoint. This approach represents a powerful tool for the valorisation of typical high quality food.

Nowadays, food quality is a frequently discussed topic, which is becoming more and more relevant for consumers, producers and regulatory institutions as well, as a consequence of the several episodes that threatened the authenticity and safety of foodstuffs. The definition of quality is a quite complex and subjective task. However, besides the fundamental requirements of health and safety, a food is perceived to be of high quality when characterized by some peculiarities, often related to typical provenance or traditions. This is particularly true for the oenological field, since wine quality is strictly linked to its history, geographical origin, raw materials and producer's "savoir faire". The European Union (EU) played a key role by recognizing the link between the product and the territory of origin as a quality attribute. The promotion and protection of typical food and beverages were carried out through the introduction of product designations (Protected Designation of Origin, PDO; Protect-

Il presente contributo è stato presentato alla XII Giornata della Chimica dell'Emilia Romagna, svoltosi il 17 dicembre 2012 presso il Dipartimento di Scienze Chimiche e Farmaceutiche dell'Università di Ferrara.

ed Geographical Indication, PGI; Traditional Speciality Guaranteed, TSG) and the concept of traceability (EC 178/2002). Traceability is defined as the ability to trace and follow a food, feed, food-producing animal or substance intended to be, or expected to be, incorporated into a food or feed, through all the stages of production, processing and distribution. The "conventional traceability" generally provides targeted information about each product or product batch, keeping track of every occurring process action. Beside this, the geographical traceability is aimed to assess the geographical origin of products. Recently, Italian institutions introduced the mandatory labelling of food with information about its (or its raw material) provenance (Decree of 3 February 2011, n° 4). Nevertheless, in most cases, the actual traceability systems are based on papery documents or certifications, which present some potential limits, such as difficulties in the availability of information and a higher risk of alteration. The possibility to trace the provenance of food on the basis of objective analytical criteria could be a valuable support for the traditional paper declarations. In particular, this scientific approach might be a powerful tool to enhance consumer confidence and represent an added value for the valorisation of typical foodstuffs which already have a high reputation. In this context, the research project "New analytical methodologies for the geographical and varietal traceability of oenological products", funded by Fondazioni in Rete per la Ricerca Agroalimentare (AGER, Agroalimentare e Ricerca, www.progettoager.it), aims to develop geographical traceability models for two Italian PDO wines, namely Lambrusco and TrentoDOC, typical of Modena and Trento districts, respectively. The analytical indicators to investigate food provenance, can be divided into two categories:

- primary indicators: variables, like the elemental pattern or the isotope abundance ratios of stable or radiogenic elements (D/H, $^{13}C/^{12}C$, $^{18}O/^{16}O$, $^{15}N/^{14}N$, $^{34}S/^{32}S$, $^{87}Sr/^{86}Sr$), which can directly relate characteristics of the territory with the same measured in the food;
- secondary indicators: variables linked to compositional properties of the food, measured by means of spectroscopic, spectrometric or chromatographic techniques, which indirectly, through an extensive characterization of the matrix, allow to identify products with the same origin.

Among the different traceability indicators, the $^{87}Sr/^{86}Sr$ isotope ratio proved to give excellent results for different types of food matrices and in particular for oenological products [1-3]. Strontium has four natural stable isotopes: ^{84}Sr, ^{86}Sr, ^{87}Sr and ^{88}Sr. Only ^{87}Sr isotope is radiogenic, thus its concentration increases over time, since it is formed by the β decay of ^{87}Rb. As a consequence, $^{87}Sr/^{86}Sr$ isotope ratio varies according to the age of the rocks and to the initial $^{87}Rb/^{87}Sr$ value, leading to a higher strontium isotope ratio in older rocks with greater rubidium content. For geographical traceability, it is worth noting that this indicator is strictly linked to the geological feature of the soil, its age and thus the geographical area of provenance. Moreover, strontium is easily assimilated by plants, as a substitute for calcium, and involved in their metabolic processes, without significant changes in the relative Sr isotope abundances. Owing to $^{87}Sr/^{86}Sr$ isotope ratio properties, it is reasonably possible to find the same indicator value in all the matrices of the investigated system (soil, plant, intermediates, final product). The proposed systematic approach is based on the synergistic use of both advanced instrumental techniques and multivariate data analysis (chemometrics) tools, in order to obtain robust and reliable traceability models. As a matter of fact, several aspects should be taken into account, i.e. the optimization of the analytical procedures for the determination of the traceability indicators, the planning of a representative sampling both for soils and food, the study of the peculiarities and variability of the indicators. Considering the great number of variables affecting most of these issues, it is noteworthy that the use of chemometrics techniques is of fundamental support to obtain a clear and comprehensive understanding.

Given the extension of the considered geographical areas (e.g. the district of Modena, considering the case of Lambrusco wine, is 2700 km^2) and the novelty and complexity of this research, a pilot study on a reduced number of samples was started. This allowed to gain a preliminary knowledge about the investigated system. First of all, a preliminary screening of the soils was performed by means of X-ray diffraction and chemometrics, in order to evaluate in a simple and relatively fast way the soil variability, considering also the influence of sampling depth and period. This approach allowed to obtain indications about the suitable soil sampling procedure (e.g. the depth of sampling, the number and the location of samples within the same farm, the period of the sampling) [4]. After that, the $^{87}Sr/^{86}Sr$ isotopic ratio was determined by means of Multi Collector ICP Mass Spectrometry in different matrices of the oenological chain (soil - branch - grape juice) to monitor the variability of the indicator in the soil and examine its behaviour during the grapevine uptake. Fig. 1 reports some results of the Lambrusco wine pilot study. Considering the graph scale and the value dispersion, which is on the fourth decimal digit, a good match is found between the isotopic values monitored in the soil fractions mimicking the bio-available part and their respective grape juices. The correlation with food matrices improves when the isotopic values of vine branches are considered. This behaviour could be explained by considering that the complexity of the soil could deeply influence the plant uptake. The possibility to use the plant as direct sampling device represents a great support, since it allows to overcome the problems associated with soil sampling, its structure and composition, as well as those related to the evaluation of the bio-available fraction of soil, namely the plant uptake. These results are certainly promising and fundamental in order to further develop a large-scale traceability model, considering a representative set of soil and food matrices.un potente strumento per la valorizzazione di prodotti tipici di qualità.

References

[1] P. Horn *et al., Z. Lebensm. Unters Forsch.*, 1993, **196**, 407.
[2] P. Horn *et al., Isotopes Environ. Health Stud.*, 1998, **34**, 31.
[3] R. Di Paola-Naranjo *et al., J. Agric. Food Chem.*, 2011, **59**, 7854.
[4] L. Bertacchini *et al., Talanta*, 2012, **98**, 178.

RIASSUNTO

Tracciabilità geografica per la valorizzazione delle produzioni enologiche

La possibilità di trovare criteri oggettivi per la tracciabilità geografica di alimenti è una sfida attuale, che può avere importanti ripercussioni sul piano sia economico sia sociale. Questo approccio rappresenta un potente strumento per la valorizzazione di prodotti tipici di qualità.

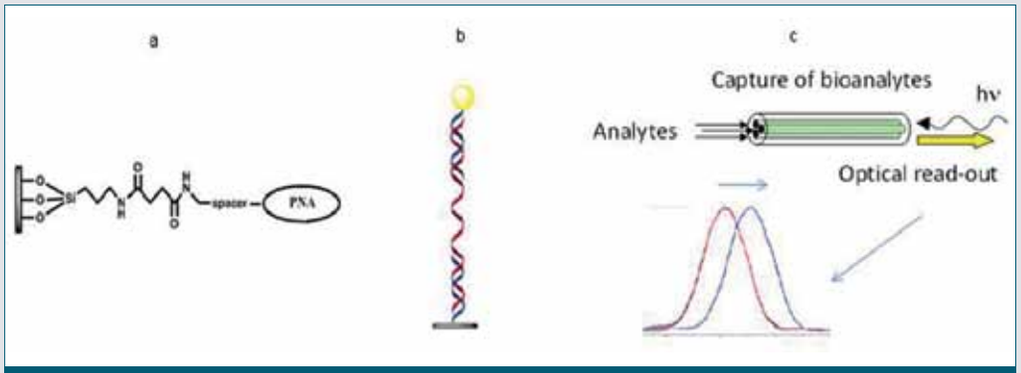

Fig. 1 - a) Scheme of the linkage of the PNA probe to the fiber internal surface; b) scheme of the sandwich-like system used for DNA detection; c) schematic summary of how measurements are performed: after the capture of bioanalytes by PNA probe, IR light coming from the laser source generates a reflection signal due to the Bragg grating, and the final wavelength shift of the reflected band is collected

[1]Alessandro Bertucci,
[1]Alex Manicardi,
[1]Emanuela Cavatorta,
[2]Alessandro Candiani,
[2]Michele Sozzi,
[2]Annamaria Cucinotta,
[2]Sara Giannetti, [2]Stefano Selleri,
[1]Roberto Corradini
[1]Dipartimento di Chimica
Università di Parma
[2]Dipartimento di Ingegneria dell'Informazione
Università di Parma
alessandro.bertucci@nemo.unipr.it

DEVELOPMENT OF NEW TOOLS FOR HIGHLY SPECIFIC NUCLEIC ACID DETECTION: PNA-MODIFIED PHOTONIC CRYSTAL FIBERS AND PNA-BASED SWITCHING PROBES

In this work, novel sensing tools based on the use of peptide nucleic acid (PNA) for biophotonic applications and for nucleic acid detection are presented. The feasibility of novel specific DNA sensing systems, based on the use of photonic crystal fibers modified with specific PNA probes is described. PNA scaffold was then used for the design of doubly modified PNAs bearing two reporter groups as new switching probes for nucleic acid recognition. Further studies about hybridization and sensing properties of these novel probes are in progress.

Peptide nucleic acids (PNAs) are oligonucleotide (ON) mimics that, due to their exceptional properties in DNA and RNA hybridization and their high chemical and biological stability, are very well suited for the detection of specific nucleic acid target sequences [1]. In this work PNAs have been used for the development of new advanced DNA detection methods.

Biophotonics represents a very attractive field of interest, integrating ICTs with biological systems and bioprobes [2]. In this field, photonic crystal fibers (PCFs), also known as microstructured optical fibers (MOFs), have the unique feature of presenting a cross-section defined by air-hole arrays running throughout the fiber, allowing to perform internal functionalization [3].

Sensing performed in these fibers exploits the evanescent tails of the guided mode field: the larger the fraction of the field that propagates as this evanescent wave, the stronger the interaction with samples placed in the holes or onto the surfaces. The presence of a Bragg grating inscribed in the core induces the formation of reflected bands that can be used to detect the presence of a biomolecule layer on the fiber capillaries, monitoring the wavelenght shift in the IR spectrum range due to variation of the total refractive index [4]. In this work, MOFs were used for the development of a novel specific DNA sensing system, based on the use of photonic crystal fibers combined with very specific PNA probes.

Internal surface derivatization was achieved using silanization with (3-aminopropyl)trietoxysilane (APTES), followed by introduction of a succinyl moiety and then by linkage to an N-terminal spacer of the PNA probe (Fig. 1a). Oligonucleotide-functionalized gold nanoparticles (ON-AuNPs) were used for signal amplification, exploiting a sandwich-like arrangement on the DNA target captured by PNA probes (Fig. 1b). First experiments were carried out with a functionalized 5-hole PCF using as target an oligonucleotide mimicking a DNA sequence bearing a single point mutation (W1282X) which is implicated in cystic fibrosis (CF) disease. The average shift of the high order wavelength for a 100 nM DNA solution was found to be

Il presente contributo è stato presentato alla XII Giornata della Chimica dell'Emilia Romagna, svoltosi il 17 dicembre 2012 presso il Dipartimento di Scienze Chimiche e Farmaceutiche dell'Università di Ferrara

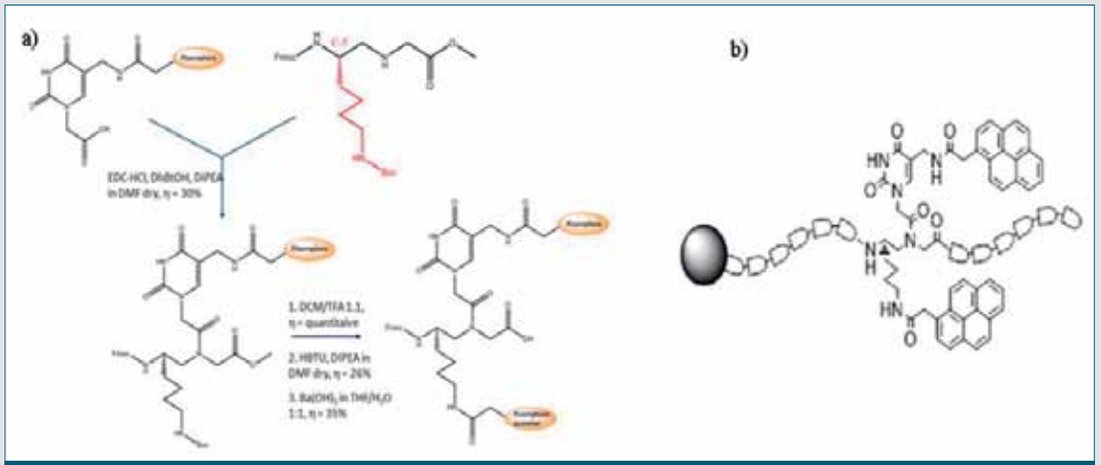

Fig. 2 - a) Synthetic approach used for the syntheses of doubly-functionalized PNA monomers; b) pyrene-modified PNA strand synthesized by solid phase synthesis

0.19±0.06 nm (n=3, RSD%=35%). The sequence-selectivity of the fiber was tested using the mis-matched oligonucleotide, corresponding to wild type DNA differing for only one base from the full-match one (FM): in this case, the total shift was of 0.05 nm, clearly much lower than that obtained using FM-DNA.

The same protocol was then carried out with a different kind of PCF, a 60-hole fiber for the detection of genomic DNA extracted from RR-GMO soy flour. Samples of 30 ng/mL concentration, containing different percentages of target GM DNA (0%, 1%, 10%) were used for the analysis and statistically different shifts were obtained for the sample containing 10% GM. To our knowledge, this was the first time a sensing system based on optical fibers allowed to perform "PCR-free" genomic DNA detection at very low concentration.

The PNA scaffold can be used for the design of new switching probes for nucleic acid detection on surfaces and in solution [5, 6]. In particular the interest was put on doubly modified PNAs bearing two reporter groups: a pyrene-based monomer-excimer probe and a fluorophore-quencher system based on the presence of the couple fluorescein-dabcyl were obtained.

First of all the synthesis of modified PNA monomer was carried out starting from 5-azidomethyluracil and a modified backbone containing a C-5 lysine chain, following the synthetic pathway schematically shown in Fig. 2. The subsequent fluorescent studies performed on the functionalized PNA monomers showed the formation of the excimer band in case of the pyrene-modified PNA and suppression of the fluorescein fluorescence in the other, thus demonstrating the interaction between the group placed on the base and that on the backbone. A doubly modified PNA sequence was then obtained exploiting solid phase synthesis both for the PNA structure and for the subsequent modifications. A PNA oligomer with a doubly-modified monomer (containing an azide moiety and the lysine side chain) corresponding to the middle thymine was obtained exploiting mixed Boc/Fmoc solid phase synthesis. Once the full PNA strand was obtained, Staudinger reaction was carried out in solid phase to create an amine from the azide; subsequently, Fmoc group was removed from the lysine side chain and coupling with 1-pyreneacetic acid was finally carried out (HBTU/DIPEA coupling) to give the doubly modified PNA oligomer. Studies about the monomer-excimer fluorescence switching properties in presence of full-complementary DNA strand, single mismatched and random sequences are currently ongoing, as well as the characterization of the duplex melting curves in these different cases. The synthesis of the fluorescein-dabcyl-modified PNA sequence will be also the next step of the work, together with a complete study of the fluorescent properties of the switching system.

Acknowledgments: This work was partly supported by grants of Italian Ministry of University and Research (MIUR) PRIN 2009 and by Italian Ministry of Agriculture (MIPAF) OLIBIO project.

References

[1] A. Bertucci, A. Manicardi, R. Corradini, Advanced Molecular Probes for Sequence-Specific DNA Recognition, in Detection of non-amplified Genomic DNA, G. Spoto, R. Corradini (Eds.), Springer, Dordrecht, The Netherlands, 2012.
[2] X. Fan, I.M. White, *Nat. Photonics*, 2011, **5**, 591.
[3] R. Corradini, S. Selleri, Photonic Crystal Fiber for Physical, Chemical and Biological Sensing, 2010, 80 in Photonic Crystal Fibers for Physical, Chemical and Biological Sensing, M. Prisco *et al.* (Eds.), Bentham Publisher, in press.
[4] A. Candiani *et al., IEEE J. Sel. Top. Quant.*, 2012, **18**, 1176.
[5] R. Corradini *et al., Curr. Top. Med. Chem.*, 2011, **11**, 1535.
[6] A. Manicardi *et al., Artif. DNA PNA XNA*, 2012, **3**, 53.

RIASSUNTO

Sviluppo di nuovi sistemi per la rivelazione ultrasensibile di acidi nucleici: fibre ottiche a cristallo fotonico funzionalizzate con PNA e "switching probes" basati su PNA modificati

In questo lavoro sono presentati nuovi sistemi di rivelazione basati sull'uso di PNA per applicazioni in biofotonica e per la costruzione di sonde altamente specifiche. Fibre ottiche a cristallo fotonico (PCF), opportunamente modificate con sonde a base di PNA, sono state utilizzate per creare sistemi ibridi di rivelazione per target di importanza nel campo biomedico e di sicurezza alimentare. La struttura del PNA è stata poi utilizzata come base per la realizzazione di PNA doppiamente modificati come nuove sonde per la rivelazione di acidi nucleici. Studi sulle proprietà di ibridazione di tali sistemi sono quindi in corso.

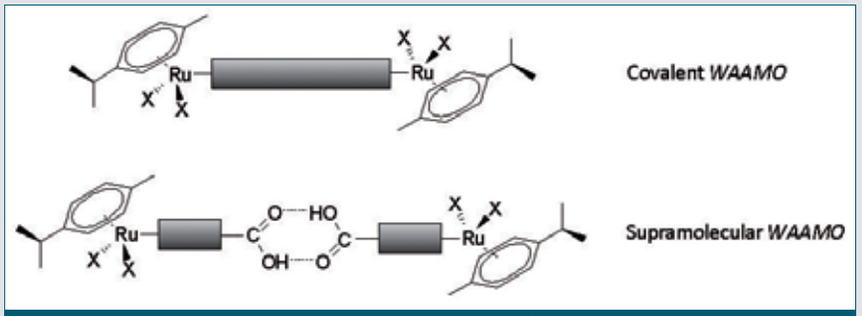

Scheme 1 - Scheme of covalent and supramolecular *WAAMO*

[1]Alessia Bacchi, [2]Susan Bourne, [1]Giulia Cantoni, [2]Gift Mehlana, [1]Paolo Pelagatti, [3]Silvia Rizzato
[1]Dipartimento di Chimica
Università di Parma
[2]Department of Chemistry
University of Cape Town (South Africa)
[3]Dipartimento di Chimica Strutturale
e Stereochimica Inorganica
Università di Milano
giulia.cantoni@nemo.unipr.it

INCLUSION PROPENSITY OF NEW WHEEL-AND-AXLE COMPLEXES BASED ON Ru(II) HALF-SANDWICH UNITS

In this contribution we present the rationalization of the solid-state packing of new organometallic materials with flexible dynamic frameworks, able to create pores on demand in order to accommodate small guest molecules. Wheel-and-axle (WAA) systems are known to be good candidates to generate inclusion compounds: they are constituted by two bulky groups (wheels) connected by a rigid linear spacer (axle). Among the complexes synthesized, [(p-cymene)Ru(3-amino-4-hydroxybenzoic acid)I_2] and {[(p-cymene)RuCl_2]$_2$[4,4'-bis-(diphenylphosphino)biphenylene]} showed an interesting propension to generate solvate forms through solid-vapour processes; the flexibility of their crystalline networks and the robustness of the supramolecular synthons involved are here analyzed.

Our interest is focused on the realization of a new class of wheel-and-axle systems, designed on the basis of half-sandwich Ru(II) organometallic building blocks (*WAAMO* = wheel-and-axle metallorganic), with the purpose of building flexible and dynamic networks with "pores on demand", similar to the 3rd generation hosts described by Kitagawa for metal organic frameworks (MOF) [1]. In this study we aim to design a host unit that in the solid state, when exposed to an external stimulus, like gas or solvent vapours, is able to undergo a conformational rearrangement in order to accommodate the guest molecules within its crystalline scaffold; moreover, this process should be completely reversible, i.e. the guest should be induced to leave the system (for example through an increase in temperature) by restoring the original structure without loss of crystallinity.

Our systems are based on a wheele-and-axle geometry [2]: they are constituted by two bulky metal-containing units at the ends, while the central spacer can be constructed either by a bidentate divergent ligand granting a covalent rigid axle (covalent *WAAMO*), or by a robust supramolecular synthon (supramolecular *WAAMO*) occurring between suitable dimerizing functions present on an organic ligand bound to the metal (Scheme 1); this irregular dumbbell shape is well known for its difficulty in achieving a unique compact stable packing, that rather may be realized by inclusion of suitable small molecules that fill the voids.

In this contribution we describe the solid-state behaviour of some new *WAAMO* complexes containing two half-sandwich [(*p*-cymene)RuX_2] (X = Cl, I) units as wheels; with regard to the supramolecular

Fig. 1 - The interconversion between **1ns** and **1·Me2CO**

Il presente contributo è stato presentato alla XII Giornata della Chimica dell'Emilia Romagna, svoltosi il 17 dicembre 2012 presso il Dipartimento di Scienze Chimiche e Farmaceutiche dell'Università di Ferrara.

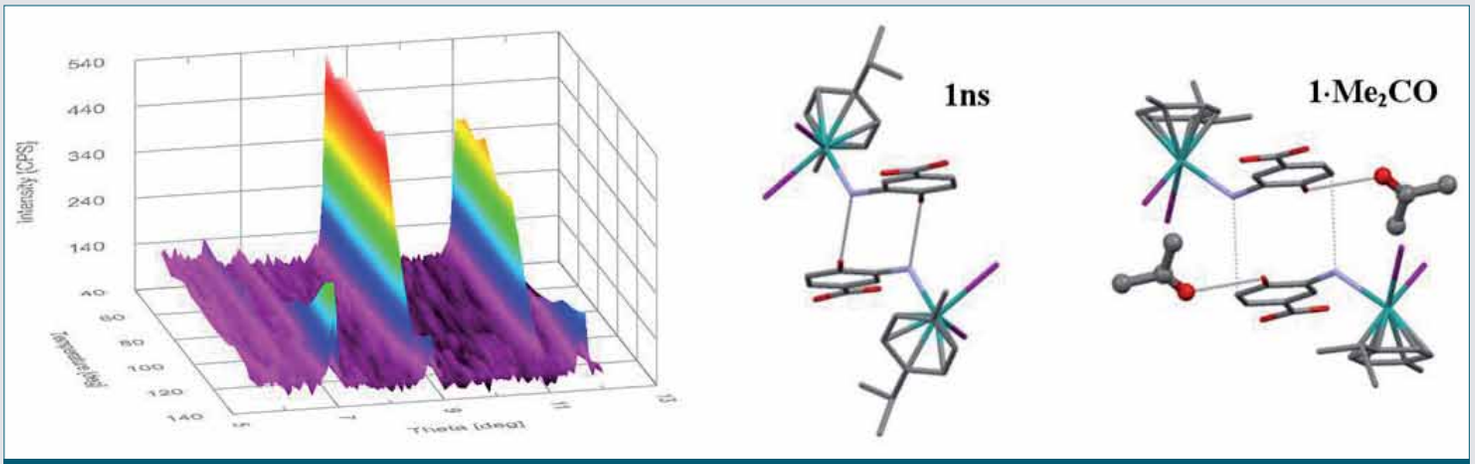

Fig. 2 - Extrusion process of **1·Me2CO** monitored by X-ray powder diffraction (left) and side view of **1ns** and **1·Me2CO**, showing the conformational rearrangements (right)

WAAMOs, interesting results have been observed for the complex [(*p*-cymene)Ru(3-amino-4-hydroxybenzoic acid)I_2] (**1**), where the central spacer is obtained by the supramolecular dimerization of the carboxylic acid functions belonging to the ligands [3] and the O-H function present on the phenyl group of the aminobenzoic ligand should function as a receptor site for hydrogen bond acceptor molecules, such as ketones.

Complex **1** was crystallized from solution in two different forms: as a non-solvate from acetonitrile (**1ns**), and as acetone-solvate from acetone (**1·Me_2CO**), with a 1:1 host:guest ratio; the analysis of their crystal packing shows in both cases the realization of the desired 3D scaffolds, with the host molecules arranged in well-structured layers, sustained by the "inverted piano-stool" motif, a supramolecular synthon typical of half-sandwich ruthenium units. In the structure of **1·Me_2CO** we observe that the carbonylic function of the acetone molecule is engaged in a hydrogen bond with the hydroxylic group belonging to the ligand.

When the microcrystalline powder of the **1ns** is exposed to acetone vapours its complete conversion to **1·Me_2CO** is observed within 1 hour at room temperature, with a strong color change from tan to black (Fig. 1).

The acetone uptake and extrusion (induced by heating) have been monitored by X-ray powder diffraction, by which it has been possible to verify that the solvation/desolvation processes occur with complete retention of crystallinity (Fig. 2, left). This evidence for a continuous transition allowed us to hypothesize a mechanism of conversion between the two forms: during the transformation from **1ns** to **1·Me_2CO** the molecular conformation changes (the Ru(*p*-cymene)I_2 group rotates about 30° around the Ru-N bond and concomitantly the *p*-cymene ring rotates around the Ru-(η^6-arene) bond axis) and at the same time the NH···I, NH···OH, and OH···I interactions characteristic of **1ns** are broken, being replaced by OH···O(acetone) and NH···π interactions in **1·Me_2CO** (Fig. 2, right).

A much lower reactivity towards gas-uptake processes was instead observed with covalent *WAAMOs* containing linear ligands such as bipy, 4-cyanopyridyne, 1,2-trans-(4-pyridyl)ethylene and 1,2-bis-(4-pyridyl)ethane [4], which are typical divergent ligands used for the synthesis of MOF materials.

In order to improve the inclusion propensity of these systems, we decided to profoundly change the nature of the central axle, by using the ligand 4,4'-bis-(diphenylphosphino)biphenylene: this molecule presents a more irregular shape which can help the formation of voids in the packing; moreover, the presence of four benzene rings in addition to the biphenylic axle gives a significant aromatic character to the resulting complex {[p-cymene)RuCl_2]$_2$[4,4'-bis-(diphenylphosphino)biphenylene]}. These two features are very promising for the realization of inclusion compounds where an hypothetic aromatic guest can be stabilized through π-π interactions or through CH-π interactions in the case of aromatic guests functionalized with aliphatic arms.

References

[1] S. Kitagawa, K. Uemura, *Chem. Soc. Rev.*, 2005, **34**, 109.
[2] A. Bacchi *et al., CrystEngComm.*, 2008, **10**, 1916.
[3] A. Bacchi *et al., Cryst. Growth Des.*, 2012, **12**, 4240.
[4] A. Bacchi *et al., Journal of Organometallic Chemistry*, 2012, **714**, 81.

RIASSUNTO

Capacità di inclusione di nuovi complessi wheel-and-axle basati su unità half-sandwich di Ru(II)

In questo contributo presentiamo la razionalizzazione del packing allo stato solido di nuovi materiali organometallici con framework flessibili e dinamici, capaci di creare pori "on demand" al fine di inglobare piccole molecole di guest. I sistemi wheel-and-axle (*WAA*) sono noti per la loro capacità di generare composti di inclusione: essi sono costituiti da due gruppi ingombranti (ruote) collegati da uno spaziatore lineare rigido (asse). Tra i complessi sintetizzati, [(*p*-cymene)Ru(3-amino-4-hydroxybenzoic acid)I2] e {[(*p*-cymene)RuCl2]2[4,4'-bis-(diphenylphosphino)biphenylene]} hanno evidenziato un'interessante propensione a generare forme solvatate mediante processi solido-vapore; la flessibilità dei loro network cristallini e la robustezza dei sintoni supramolecolari coinvolti verranno qui di seguito analizzati.

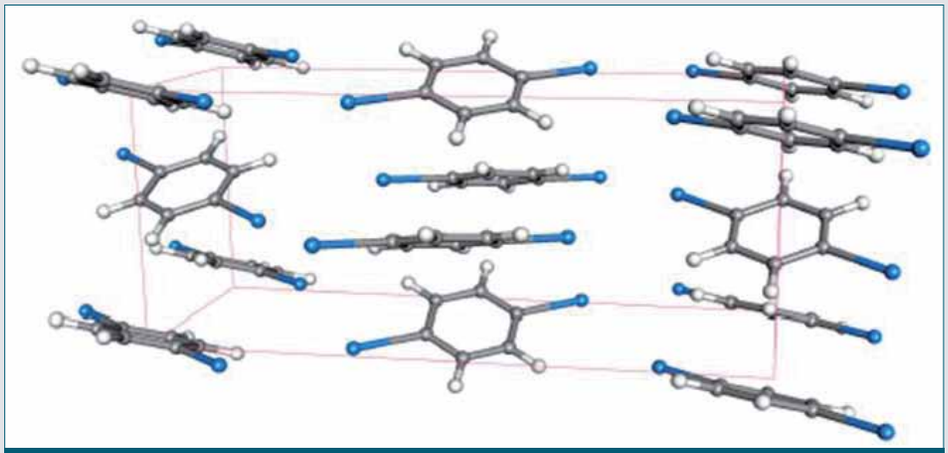

Fig. 1 - p-DIB molecular crystal (α-phase) - view of the *ab* plane

Davide Presti, Alfonso Pedone, Maria Cristina Menziani
Dipartimento di Scienze Chimiche e Geologiche
Università di Modena e Reggio Emilia
davide.presti@unimore.it

COMPUTATIONAL PREDICTION OF MOLECULAR CRYSTAL POLYMORPHISM IN *p*-DIIODOBENZENE: ON THE ABILITY OF DISPERSION-CORRECTED DFT CALCULATIONS

This contribution reports the results of periodic Density Functional Theory (DFT) calculations employing the PBE, PBE0 and B3LYP functionals coupled with different dispersion-correction schemes (-D and -TS), as applied to the para-diiodobenzene (p-DIB) molecular crystal. We show that DFT-TS calculations successfully predict the relative stability and the structures of the α and β phases of p-DIB.

Periodic Density Functional Theory (DFT) calculations employing the PBE, PBE0 and B3LYP functionals coupled with different dispersion correction schemes (-D and -TS) have been applied to *para*-diiodobenzene (*p*-DIB) molecular crystal (Fig. 1) in order to determine how they perform in reproducing the energetic and crystal geometry of its two well known polymorphs.

Our results [1] show that, when properly corrected, DFT calculations successfully predict the relative stability of the two phases α and β at zero temperature, ΔE=E(α)-E(β), in good agreement with Diffusion Monte-Carlo (DMC) calculations [2]. The comparison between ΔE (Fig. 2), obtained with the PBE and B3LYP functional corrected with the -TS and -D schemes shows that the latter approach provides values which are almost twice than that predicted by the TS scheme. The PBE-TS and PBE-D functionals in conjunction with norm-conserving pseudopotentials (NCPPs) has also been tested and yielded the a-phase more stable than the β one of 38 and 63 meV, respectively. However, these data alone confirm that all of the corrected functionals could be employed to predict the most stable form of apolar molecular crystal, such as p-DIB.

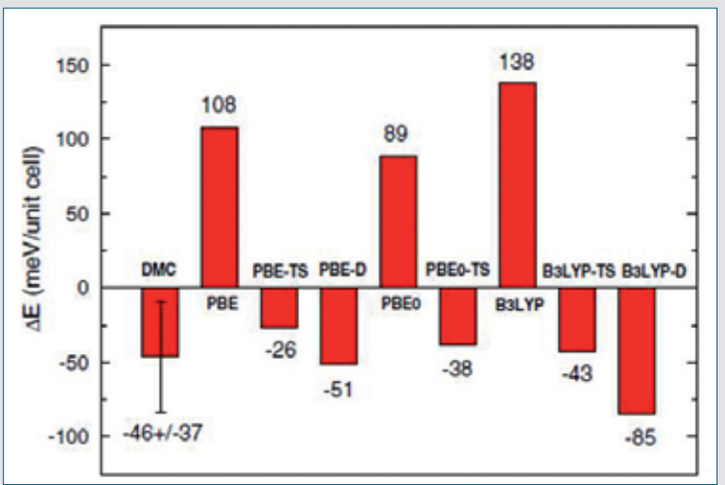

Fig. 2 - Energy differences between the α and β phases of *p*-DIB computed with the three PBE, PBE0 and B3LYP functionals with and without the -TS and -D empirical dispersion corrections. The result obtained by Hongo *et al.* [2] by means of DMC (for which the error bar is also shown) is reported for comparative purpose

Il presente contributo è stato presentato alla XII Giornata della Chimica dell'Emilia Romagna, svoltosi il 17 dicembre 2012 presso il Dipartimento di Scienze Chimiche e Farmaceutiche dell'Università di Ferrara.

Method	α-phase				β-phase				ΔE
	a	b	c	V	a	b	c	V	(meV)
PBE	17.842 (5.0)	8.815 (20.4)	6.104 (0.4)	974 (26.8)	17.333 (1.4)	8.958 (20.1)	6.189 (0.01)	961 (22.4)	+40.7
PBE-TS	17.020 (0.1)	7.14 (-2.5)	6.164 (-0.1)	749 (-2.5)	17.136 (0.3)	7.289 (-2.3)	6.110 (-0.7)	763 (-2.8)	-47.7
PBE-D	16.924 (-0.4)	6.856 (-6.3)	5.957 (-3.4)	691 (-10.0)	17.145 (0.3)	6.956 (-6.2)	5.902 (-4.1)	705 (-10.2)	-49.2
Expt.	17.000	7.323	6.168	768	17.092	7.461	6.154	785	-

Tab. 1 - Optimized lattice parameters (Å) and unit cell volume (Å3) for the two polymorphs of *p*-DIB evaluated using the PBE, PBE-TS and PBE-D functionals and compared with experimental values. The latter have been obtained at 298 and 333 K for the α and β forms, respectively [5]. Relative errors are reported in parenthesis

A better discrimination of which of the dispersion corrections provides the best results is obtained by testing the functionals in predicting the structure of the two crystalline phases. The results reported in Tab. 1 show that after full geometry optimization, the PBE functional gives the incorrect sign for ΔE and too large unit cell volumes, due to the lack of attractive vdW interactions. Interestingly, the PBE-TS results are in very nice agreement with the experimental data showing a relative error on the unit cell volume below 2.8%, while the PBE-D functional markedly reduces the cell parameters leading to a very compact structure, with relative errors greater than 10% on the cell volume, because of a severe contraction along the *b* and *c* axis. This is depicted in Fig. 3, where the optimized PBE-D and PBE-TS crystal structures of the a polymorph are superimposed to the experimental ones. The figure shows that the packing of the *p*-DIB molecules along the *b* axis is governed by the interactions between the p electron density on the benzene rings and the hydrogen atoms of a benzene molecule in an overlying molecular layer. The PBE-TS functional better reproduces these interactions with respect than the PBE-D functional.

It should be emphasized that the experimental data have been collected at 298 and 333 K for the α and β forms, respectively [5] while our calculations refer to 0 K. A proper account of thermal effect would certainly improve the agreement with experiments since the population of excited vibrational states would lead to a less compact structure.

Our work has demonstrated that, among the two dispersion corrections employed, the recently proposed Tkatchenko and Scheffler (TS) [3] scheme performs much better than the original scheme (D) proposed by Grimme [4]. This is imputable to the accurate *nonempirical* method used to obtain the dispersion coefficients in the former approach. These coefficients, in fact, can vary considerably depending on the chemical environment in which an atom is embedded, and the original parameterization proposed by Grimme is not able to capture such differences. In conclusion, the PBE-TS functional can be safely used to predict the relative stabilities and structural packing of organic molecular crystals with a relatively low computational cost with respect to more sophisticated quantum-mechanical methods.

Acknowledgements: The Ph.D. Grant of Davide Presti is supported by Ministero del Lavoro e delle Politiche Sociali, Consortium SPINNER2013, Regione Emilia-Romagna and the European Social Fund.

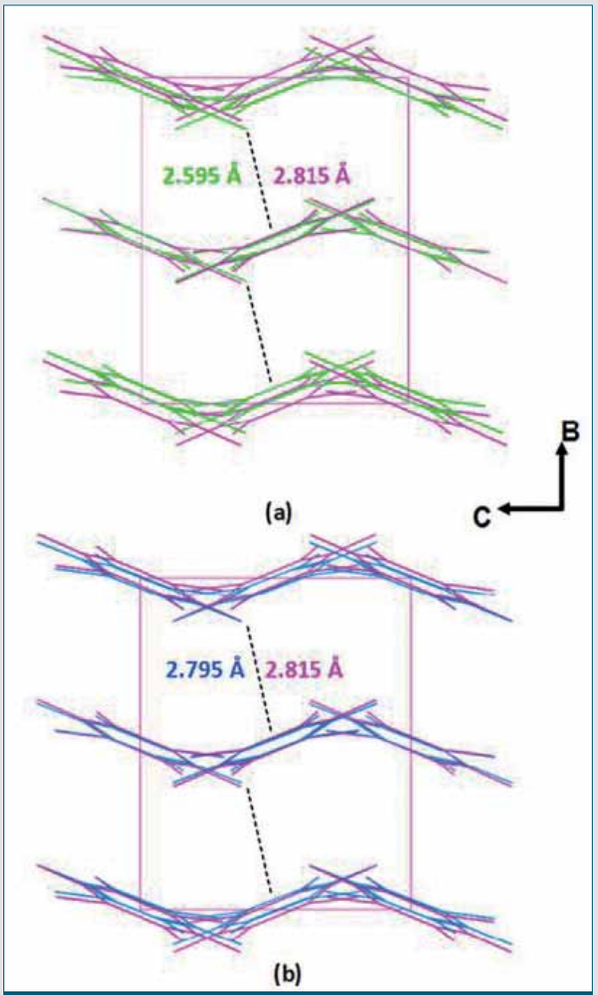

Fig. 3 - View of the *bc* plane of the optimized (a) PBE-D (light green sticks) (b) PBE-TS (blue sticks) α-form of *p*-DIB molecular crystal superimposed to the experimental structure (purple sticks). The H-π interaction between an H atom of the *p*-DIB molecule and the electron density on the benzene ring is shown by the black dashed line

References

[1] A. Pedone, D. Presti, M.C. Menziani, *Chem. Phys. Lett.*, 2012, **541**, 12.
[2] K. Hongo *et al., J. Phys. Chem. Lett.*, 2010, **1**, 1789.
[3] A. Tkatchenko, M. Scheffler, *Phys. Rev. Lett.*, 2009, **102**, 073005.
[4] S. Grimme, *J. Comput. Chem.*, 2006, **27**, 1787.
[5] X. Alcobé *et al., J. Solid State Chem.*, 1994, **110**, 20.

RIASSUNTO

Predizione computazionale sul polimorfismo del cristallo molecolare di p-diiodobenzene: accuratezza dei metodi di calcolo DFT con correzione alla dispersione

In questo contributo riportiamo i risultati ottenuti attraverso calcoli periodici facenti uso della Teoria del Funzionale della Densità (DFT), con i funzionali PBE, PBE0 e B3LYP accoppiati con due differenti schemi di correzione alla dispersione (-D e -TS), applicati allo studio del cristallo molecolare di *para*-diiodobenzene (*p*-DIB). Abbiamo dimostrato che i calcoli DFT-TS sono in grado di predire con successo la stabilità relativa e le strutture sperimentali delle fasi α e β del *p*-DIB.

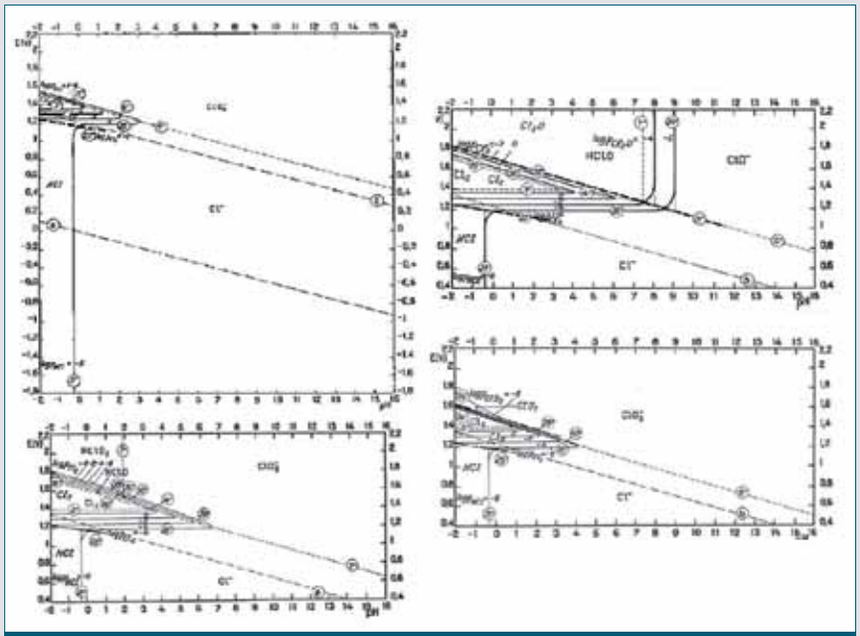

Fig.1 - Stability diagrams of oxy-chlorinated species at 25 °C

Stefano Neodo[1], Davide Rosestolato[2]
[1]nCATS, Engineering Sciences, University of Southampton (UK)
[2]Dipartimento di Scienze Chimiche e Farmaceutiche Università di Ferrara
rssdvd@unife.it

INVESTIGATION ON THE ACTIVE CHLORINE PRODUCTION FROM DILUTE CHLORIDE SOLUTIONS AND ELECTROCHEMICAL REACTIVITY OF THE SIDE-PRODUCTS

The electrolytic process of dilute aqueous chloride solutions was studied at different electrodes and experimental conditions. The time evolution of Cl-related species (i.e. ClO^-, ClO_2^-,...), as well as their faradic efficiency, were investigated to understand their mechanisms of generation and consumption.

Due to their high reactivity, low production cost and relative ease of synthesis, activated chlorine *(A.C.)* solutions have been widely used to date [1, 2] as effective biocides for disinfection of potable, industrial and agro-industrial waters [3], inhibition and removal of biofouling products [4], sanification of hospital environments and sterilization of medical utensils [5]. During the electrolytic production of *A.C.* solutions, a maximization of the chlorine yield, with the simultaneous minimization of undesired by-products, is essential to achieve the best results in terms of sterilization and control of pollutant concentrations.

The Chlorine Evolution Reaction (ClER), involved in the synthesis of *A.C.*, appears as a simple reaction when looking at eq. 1:

$$2Cl^- \rightarrow Cl_2 + 2e \qquad E°=1.35 \text{ V vs. SHE} \qquad (1)$$

Conversely, the chemical equilibria of the water-chlorine system and the possible electrochemical generation of by-products suggest that the system is complex, deserving further investigation.

A first thermodynamic information about the chlorine-water system can be extracted from the Pourbaix diagrams [6] reported in Fig. 1.

In addition, the possible generation of oxy-chlorinated species with different oxidation states depends also on kinetic aspects, which involve both the chemical and the electrochemical synthetic paths. For these reasons, the electrode properties play a primary role in this kind of applications. Different materials can be taken into consideration, including *e.g.* platinum, DSA® (based on iridium- or ruthenium-oxide) or even the less conventional boron-doped diamond (BDD) electrodes; each material has its own characteristics that can be suitable or not for water treatment. Platinum is a good catalyst for both ClER and is characterized by a high stability, but its cost is a serious drawback for a real application, especially if large electrode areas are required. Iridium- and ruthenium-oxide-based electrodes, deposited on titanium supports, are relatively cheaper than Ti-supported platinum, while maintaining a high catalytic activity with respect to chlorine and oxygen electro-generations. In particular, anodes based on IrO_2 are particularly suitable when high current densities have to be applied, because of their incomparable stability; on the contrary, $Ru^{(VI)}$ and $Ru^{(VIII)}$ oxo-complexes are formed at high anodic potentials (the former is water-soluble, while the latter is volatile and toxic), and specifically stable oxide mixtures have to be considered.

In the present work, the electrolytic process of dilute aqueous chloride solutions (0.07 M) was investigated at $Ti/RuO_2{\bullet}2SnO_2$ and Ti/Pt electrodes,

Il presente contributo è stato presentato alla XII Giornata della Chimica dell'Emilia Romagna, svoltosi il 17 dicembre 2012 presso il Dipartimento di Scienze Chimiche e Farmaceutiche dell'Università di Ferrara.

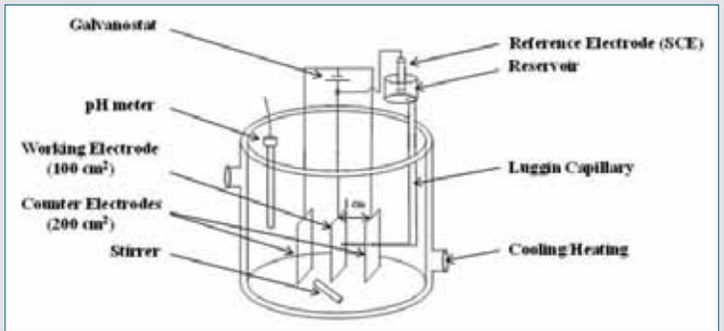

Fig.2 - Scheme of the apparatus used for controlled electrolyses

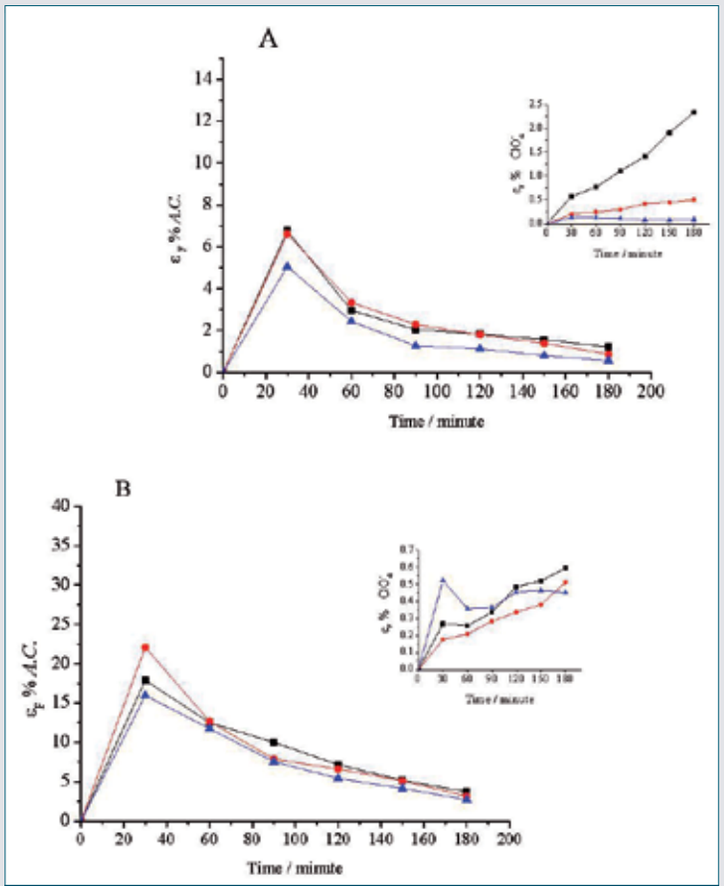

Fig. 3 - Current efficiencies for active chlorine and perchlorate (inset) vs. time, estimated for electrolyses carried out on (A) Ti/Pt and (B) $Ti/RuO_2{\cdot}2SnO_2$, in 0.07 M NaCl at 1500 Am^{-2}, when working at 10 (black), 25 (red) and 65 (blue) °C

at different values of current density (250, 750 and 1500 Am^{-2}), temperature (10, 25 and 65 °C) and electrolysis time (0-180 minutes) [8].

The time evolution of chlorine-related species (*i.e.* active chlorine, chlorite, chlorine dioxide, chlorate and perchlorate), as well as their faradic efficiency, was investigated to understand whether their formation and consumption was either chemical or electrochemical. The electrolysis apparatus is shown in Fig. 2; the working electrode (WE) has been located between two titanium plates (counter electrodes), and its potential was measured with respect to a standard calomel (SCE, reference) immersed in a reservoir hydraulically linked through a Luggin capillary that was located in the proximity of the WE surface.

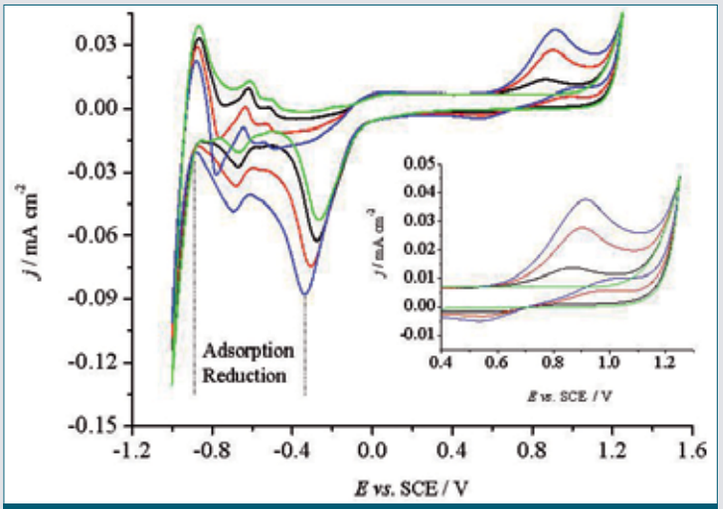

Fig. 4 - Cyclic voltammograms of Pt at 0.1 Vs^{-1} in (green) 0.1 M $NaClO_4$ and in the presence of (black) 1.0 mM, (red) 2.0 mM and (blue) 3.0 mM $NaClO_2$, at pH 9.0. An enlargement of the anodic section is shown in the inset

Working electrode surface area was 100 cm^2. During the electrolytic process, the solution was vigorously stirred and steadily maintained at the desired *T* (*i.e.* 10, 25 or 65 °C) and j (250, 750 or 1500 Am^{-2}). The overall duration of each test was 180 minutes; the pH and electrode potential were determined at 30 minutes intervals.

Furthermore, aliquots of 5 mL were also sampled and chemically analyzed to obtain information regarding *A.C.*, chlorite, chlorine dioxide, chlorate and perchlorate bulk concentrations. *A.C.*, chlorite, chlorine dioxide, and chlorate concentrations were determined by a iodometric method [7], while the perchlorate content was assessed by ion chromatography (IC), using a DX 120 Dionex equipped with an Ion Pack AS16 column (4x250 mm) and a 1 mL injection loop.

Further electrochemical tests, in particular cyclic voltammograms, were carried out in a single-body, three-electrode cell, where a SCE and a large area platinum-mesh served as reference and auxiliary electrodes, respectively. A platinized Pt wire was used as the working electrode, and measurements were performed using a 0.1 M $NaClO_4$ solution as the supporting electrolyte. The electrolyses of diluted chloride solutions, carried out using the single-body cell in Fig. 2, showed the possibility of obtaining active chlorine solutions with a variable content of by-products, whose concentrations largely depended on the process variables (time, temperature and anode material). Significant differences in the process efficiencies of Ti/Pt and $Ti/RuO_2{\bullet}2SnO_2$ were attained, values approximately 3-fold higher being assessed for the DSA-type electrode with respect to the platinum anode, throughout all the galvanostatic tests, thus highlighting the excellent catalytic activity of the $Ti/RuO_2{\bullet}2SnO_2$ electrode (Fig. 3). The formation of perchlorate is favoured by high electrode potentials and low temperatures. Regarding the chlorite and the chlorine dioxide species, their low concentration levels, assessed throughout all electrolysis tests, indicated a depletion process potentially driven by both an electrochemical and a chemical routes. In order to establish which process prevailed, cyclic voltammetry tests were carried out in chlorite-containing solutions, at different potential scan rates and mass-transfer regimes.

Collected data (Fig. 4) suggested a high reactivity of investigated bulk species toward both the anodically and cathodically polarized surfaces; in particular, the presence of peak A1 (oxidation of ClO^-) implies a facile reduction of ClO_2^- to ClO^- (eq. 2) and Cl^- (eqs. 3-4):

$$ClO_2^- + H^+ + e \rightarrow ClO^- \quad (2)$$
$$ClO^- + H_2O + e \rightarrow Cl_{ads} + 2OH^-_{ads} \quad (3)$$
$$Cl_{ads} + e \rightarrow Cl^- \quad (4)$$

The above shown results witness for the important role played by the electrode material in processes involving simultaneous chlorine and oxygen evolution reaction, and prompt further investigation in order to optimize the process and allow its implementation in potable water treatment.

References

[1] H. Gallard, U. Von Gunten, *Environ. Sci. Technol.*, 2002, **36**, 884.
[2] M.C. Dodd *et al., Environ. Sci. Technol.*, 2006, **40**, 3285.
[3] C. Feng *et al., Bioresource Technol.*, 2004, **94**, 21.
[4] D. De Beer *et al., Appl. Environ. Microb.*, 1994, **60**, 4339.
[5] J. Lenz *et al., Int. J. Hyg. Environ. Health*, 2010, **213**, 198.
[6] M. Pourbaix, N. De Zoubov, J. Van Muydler, Atlas d'équilibres électrochimiques (Paris, Gauthier-Villars & C^ie, éditeur-imprimeur-libraire, 55, Quai des Grands-Augustins, 55, 1963).
[7] Caffaro Monografie, Capitolo: Il biossido di cloro, 2002, pp. 72-75.
[8] S. Neodo *et al., Electrochimica Acta*, 2012, **80**, 282.

RIASSUNTO

Studio sulla produzione di cloro attivo a partire da soluzioni diluite di cloruri e sulla reattività elettrochimica dei sottoprodotti

Nel presente lavoro è stato studiata l'elettrolisi di soluzioni diluite in cloruri usando differenti materiali elettrodici in diverse condizioni sperimentali. L'efficienza faradaica durante il tempo di elettrolisi ha permesso di ottenere informazioni sul meccanismo di generazione e di consumo delle specie ossiclorurate.

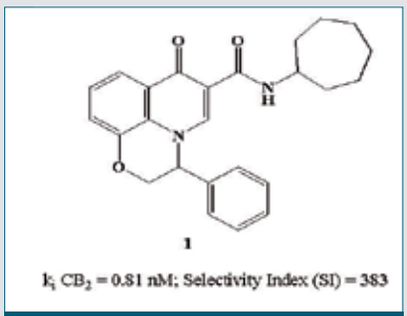

Fig. 1 - *N*-cyclohexyl-3,7-dihydro-7-oxo-3-phenyl-2*H*-[1,4]oxazino[2,3,4-*ij*]quinoline-6-carboxamide

Pier Giovanni Baraldi[1], Giulia Saponaro[1], Delia Preti[1], Stefania Baraldi[1], Emanuela Ruggiero[1], Pier Andrea Borea[2], Mojgan Aghazadeh Tabrizi[1]
[1]Dipartimento di Scienze Farmaceutiche
Università di Ferrara
[2]Sezione di Farmacologia, Dipartimento di Medicina Clinica e Sperimentale
Università di Ferrara
emanuela.ruggiero@unife.it

7-OXO-[1,4]OXAZINO[2,3,4-*IJ*] QUINOLINE-6-CARBOXAMIDES AS SELECTIVE CB_2 CANNABINOID RECEPTOR LIGANDS: STRUCTURAL INVESTIGATION AROUND A NOVEL CLASS OF FULL AGONISTS

Cannabinoid receptor agonists have gained attention as potential therapeutic targets of inflammatory and neuropathic pain. Here, we report the identification and optimization of a series of 7-oxo-[1,4]oxazino[2,3,4-ij]quinoline-6-carboxamide derivatives as a novel chemotype of selective cannabinoid CB_2 receptor agonists. In cAMP assays, the novel series behaved as agonist, exhibiting functional activity at the human CB_2 receptor.

Cannabinoids are the pharmacologically active components of cannabis, and are known to mediate some of their actions through the cannabinoid receptors. Two distinct cannabinoid receptors named CB_1 and CB_2 have been cloned and characterized from mammalian tissues. The CB_1 receptor is abundantly expressed in the central nervous system (CNS) and is responsible for the psychotropic side effects. The cannabinoids CB_2 receptor is mainly found in cells of the immune system and it is upregulated in the CNS under pathological conditions. Cannabinoid CB_2 receptors have gained attention as potential therapeutic targets in the management of neuropathic pain. Significant drug discovery efforts have been directed toward developing and characterizing CB_2-selective agonists.

Il presente contributo è stato presentato alla XII Giornata della Chimica dell'Emilia Romagna, svoltosi il 17 dicembre 2012 presso il Dipartimento di Scienze Chimiche e Farmaceutiche dell'Università di Ferrara.

Within a research program in order to identify novel CB_2-agonists, we designed a hybrid chemical structure that incorporated the structural features of known cannabinoid ligands. The new 7-oxo [1,4]oxazino[2,3,4-ij]quinoline-6-carboxamides, such as compound **1** (Fig. 1) were synthesized and tested in binding assays, exhibiting high affinity and selectivity for the CB_2 receptor. This preliminary result led us to initiate a pharmacophore exploration and optimization effort around the oxazinoquinolin-4-one central scaffold. The target 7-oxo-[1,4]oxazino[2,3,4-*ij*]quinoline-6-carboxamides were prepared following two synthetic routes, depending upon the availability of the requisite α-halo ketone or amino alcohol to form the desired substitution patterns at C-2 and C-3 of the oxazine moiety.

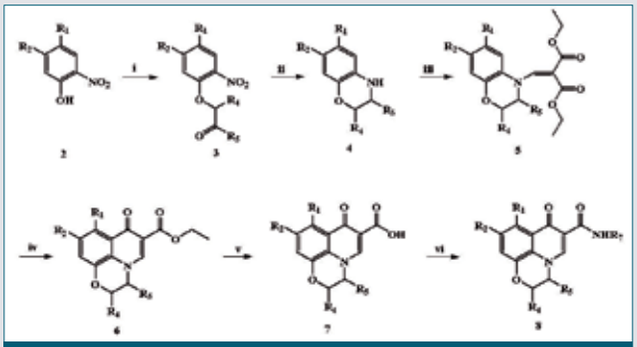

Scheme 1 - Reagents and conditions: (i) α-halo ketone, K_2CO_3, acetone (anhydrous), rt, 16 h; (ii) H_2 (4 atm), 10% Pd/C, MeOH, 4h; (iii) diethyl(ethoxymethylene)malonate, 140 °C, 2 h; (iv) poly(phosphoric acid), 140 °C, 1 h; (v) 10% NaOH, CH3OH, 80 °C, 1h; (vi) amine, EDC, HOBt, DMF, rt, 6 h or amine, DIEA, HBTU, DMF, rt, 16 h

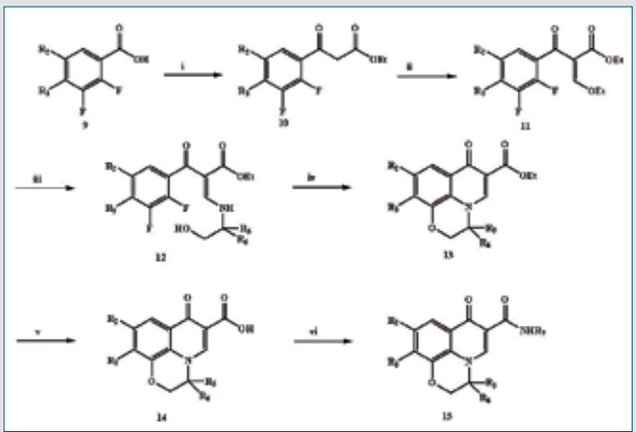

Scheme2 - Reagents and conditions: (i) CDI, THF, $(C_2H_5O)_2Mg$, monoethyl malonate, rt, 16 h; (ii) $CH(OEt)_3$, Ac_2O, 110 °C, 3 h; (iii) appropriate (*R*)-,(*S*)-, or (*R,S*)-amino alcohol, CH_2Cl_2, rt, 1 h; (iv) K_2CO_3, DMF, 130 °C, 7 h; (v) 10% NaOH, CH_3OH, 80 °C, 1 h; (vi) amine, EDC, HOBt, DMF, rt, 6 h or amine, DIEA, HBTU, DMF, rt, 16 h

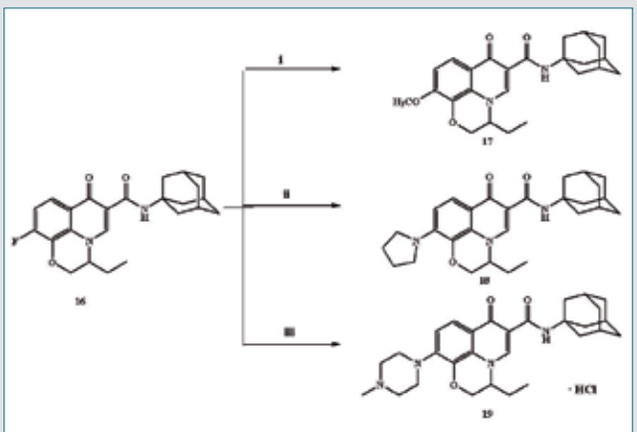

Scheme 3 - Reagents and conditions: (i) CH_3ONa, THF, 50 °C, 16 h; (ii) K_2CO_3, DMF, pyrrolidine, 100 °C, 10 h; (iii) K_2CO_3, DMF, 1-methylpiperazine, 100 °C, 10 h, then 1,4-dioxane saturated with HCl gas, 0 °C, 30 min

The benzoxazine precursors were prepared in two steps by deprotonation of 2-nitrophenols **2**, followed by alkylation with the appropriate α-halo ketones to give nitro ketones **3**. In the second step, catalytic hydrogenation of the nitro ketones **3** using 10% palladium-on-carbon in methanol gave the intermediates **4** by a concomitant reduction-reductive amination sequence. Subsequent reaction with diethyl (ethoxymethylene)-malonate (DEEM) at 140 °C furnished the corresponding methylenemalonate derivatives **5** in 70-90% yields. A thermally induced cyclization of **5** in poly(phosphoric acid) (PPA) for 1 h afforded the oxazinoquinoline ester derivatives **6** in 75-95% yields. After saponification of the ethyl ester functionality of compounds **6**, the resulting carboxylic acids **7** were engaged in an amidation reaction with the appropriate amines under peptide coupling conditions to afford the target amide compounds **8** (Scheme 1).

The synthesis of target compounds (general structure **15**) was accomplished using a procedure similar to that utilized for preparing optically active ofloxacines (Scheme 2). Ethyl 3-oxopropanoates **10** were prepared from the corresponding benzoic acids **9** by reaction with carbonyldiimidazole (CDI) in THF to afford the imidazolide, followed by condensation with the magnesium salt of monoethyl malonate under essentially neutral conditions (90% yield). Subsequent condensation with triethyl orthoformate in refluxing acetic anhydride produced the ethyl 2-(ethoxymethylene) propionates **11**. These intermediates were reacted with the appropriate amino alcohols in dry methylene chloride in an addition-elimination sequence to afford the intermediates **12**. Cyclization using potassium carbonate (K_2CO_3) in dimethylformamide (DMF) at 130 °C followed by saponification afforded the carboxylic acids **14** that were coupled with the appropriate amines to afford the final compounds. Similarly, reaction of intermediate **11** with the appropriate (*R*)- or (*S*)-amino alcohol led to the preparation of the corresponding enantiomerically pure derivatives (**3**).

The target compounds **17-19** were obtained by displacement of the fluorine substituent at C-10, treating the amide **16** with different nucleophiles (sodium methoxide, pyrrolidine, *N*-methylpiperazine) in alkaline conditions (Scheme 3). The 4-methylpiperazine derivative **19** was converted to the hydrochloride salt by treatment with 1,4-dioxane saturated with gaseous hydrogen chloride.

An initial set of 12 compounds was synthesized possessing an aromatic moiety (phenyl or 4-tolyl) at C-3 of the scaffold. The substituents on the carboxamide moiety at C-6 were initially selected on the basis of other known cannabinoid pharmacophores, that is to say cyclohexyl, cycloheptyl and adamantan-1-yl derivatives. In this group the most potent and selective compound was **1**, bearing a cycloheptyl residue on the carboxamide moiety and a unsubstituted phenyl at C-3 (k_iCB_2=0.81 nM; Selectivity Index (SI) = 383). Encouraged by this notable result, we decided to extend the structure-activity relationship (SAR) study by replacement of the C-3 phenyl ring with a series of aliphatic moieties to evaluate the effect of the chain length and branching.

In this second series we found that 18 out of 23 compounds showed k_iCB_2<65 nM. These amazing affinity values led us to increase the selectivity index.

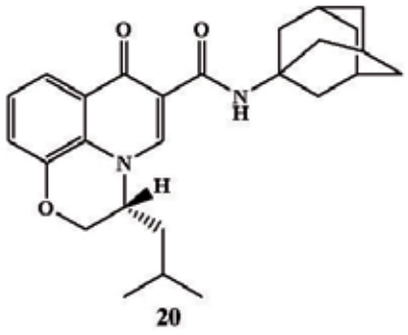

Fig. 2 - (*R*)-(+)-*N*-Adamant-1-yl-3,7-dihydro-3-isobutyl-7-oxo-2*H*-[1,4]-oxazino[2,3,4-*ij*] quinoline-6-carboxamide

Therefore, within the 3-ethyl series, which was found to have higher selectivity towards CB_2 receptor other than the other tested compounds, we examined the effect on affinity and selectivity of structural modifications at the carboxamide side chain. Optimal activity and selectivity in this group were obtained with the 5-methylhexan-2-yl carboxamide chain (hk_iCB_2=15.8 nM, SI>633). These data show that affinity and selectivity for the CB_2 receptor are quite sensitive to modifications of the 6-carboxamido group. Nevertheless, we reached the highest levels of selectivity by introducing a methoxy, *N*-methylpiperazine and especially a pyrrolidine group on C-10 of the scaffold [**18** (k_iCB_2=10.5 nM, SI>1231)]. Finally, we noticed that the presence of a *gem*-dimethyl group on C-3 significantly affected selectivity. This result suggested the possibility of a difference between the two receptor subtypes in the stereofacial preference for substituents at this position. To evaluate this possibility, we prepared a number of compounds as single enantiomers rather than racemic mixtures. Recognizing that a significant enhancement in both affinity and selectivity has been seen only with (*R*)-enantiomeres, and especially with (*R*)-3-methyl derivatives, we hypothesized that introducing a methylene spacer between the oxazine nucleus and the alkylic moiety may led to further enhancements in affinity and selectivity. This led to the synthesis and evaluation of **20** (Fig. 2), the enantiopure derivative bearing an isobutyl moiety at C-3. Indeed, this compound was found to bind to the CB_2 receptor with high affinity and exceptional selectivity (k_i=9.24 nM; SI>1082).

The potency of the novel compounds was measured in functional assays, with high potency values (represented by IC_{50}) that are closely correlated with the high affinity values (expressed as k_i), revealing that the novel series behaves as CB_2 receptor agonists. This novel series of compounds offers an attractive starting point for further optimization and represents novel pharmacological tools to evaluate the therapeutic potential of CB_2 agonists in various disease settings, especially inflammatory pain.

RIASSUNTO

7-Osso-[1,4]ossazino[2,3,4-ij]chinolin-6-carbossamidi come ligandi selettivi per il recettore CB_2 dei cannabinoidi: studio strutturale riguardo una nuova classe di agonisti pieni

L'impiego terapeutico di ligandi per i recettori CB dei cannabinoidi è al centro di numerosi studi da diversi anni, in particolar modo per il trattamento del dolore neuropatico. In questo lavoro abbiamo riportato la sintesi di un nuovo nucleo 7-osso-[1,4]ossazino[2,3,4-*ij*]chinolin-6-carbossiammidico come chemotipo di agonisti selettivi per il recettore CB_2 dei cannabinoidi.

Istruzioni per gli Autori

La Chimica e l'Industria è una rivista di scienza e tecnologia e di informazione per i chimici. Nella rubrica "Attualità" ospita articoli o comunicati brevi su argomenti di interesse rilevante per tutti coloro che operano nella chimica, richiesti dalla redazione o ricevuti come lettere al direttore. Nella sezione "Science and Technology" pubblica in inglese monografie scientifiche di chimica, ingegneria chimica e tecnologie farmaceutiche, concordate o richieste dal comitato scientifico o dalla redazione. Nella sezione "Chimica e..." ospita articoli in italiano o in inglese di carattere applicativo, tecnologico e informativo per tutti i settori rilevanti della chimica.

Testi

I testi possono essere trasmessi via e-mail, completi di tabelle e figure, con chiara indicazione dei nomi degli autori, scrivendo per esteso anche il nome di battesimo, gli Istituti o Enti presso i quali svolgono la loro attività e relativo indirizzo. Va allegato inoltre un breve riassunto del testo sia in italiano sia in inglese (max 300 battute). I testi dovranno essere contenuti in non più di 30.000 battute per quanto riguarda la sezione "Science and Technology", e non più di 16.000 battute per quanto riguarda la sezione "Chimica e...". Il numero complessivo di tabelle e figure non dovrebbe essere superiore a 10 per la sezione "Science..." e a 5 per la sezione "Chimica e...". Tutti gli articoli dovranno essere corredati di un'immagine esplicativa dell'argomento da poter utilizzare come foto di apertura. Il titolo non dovrà essere lungo più di 30 battute.

Immagini, schemi, figure vanno inviate in formato jpg, tiff o gif in file separati. Si raccomanda di uniformare la lingua delle immagini a quella del testo.

I richiami bibliografici (non più di 30-35), da citare all'interno del testo, devono essere numerati progressivamente, con numeri arabi tra parentesi quadre. La bibliografia va riportata in fondo al testo secondo gli esempi:

[1] D.W. Breck, Zeolite Molecular Sieves, J. Wiley, New York, 1974, 320.

[2] R.D. Shannon, *Acta Crystallogr.*, 1976, **32**, 751.

[3] U.S. Pat. 4.410.501, 1983.

[4] Chemical Marketing Reporter, Schnell Publ. Co. Inc. (Ed.), June 15, 1992.

[5] G. Perego *et al.*, Proceedings of 7th Int. Conf. on Zeolites, Tokyo, 1986, Tonk Kodansha, Elsevier, Amsterdam, 129.

La redazione invita inoltre gli Autori ad inviare in allegato (fuori testo) con gli articoli anche fotografie o illustrazioni relative al contenuto, sia di tipo simbolico sia descrittivo, per migliorare l'aspetto redazionale e comunicativo (la direzione se ne riserva comunque la pubblicazione). Tutto il materiale deve essere inviato per e-mail a: dott. Anna Simonini, anna.simonini@soc.chim.it